

RELEASE DATE

JUN 6 1957

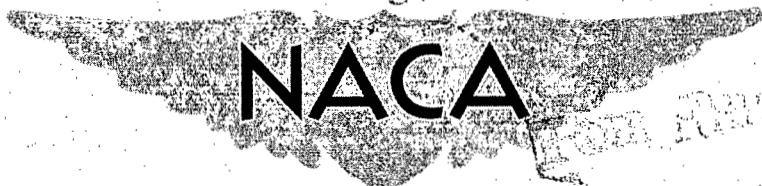
~~CONFIDENTIAL~~

Copy
RM L57D23b

NACA RM L57D23b

UNCLASSIFIED

21



RESEARCH MEMORANDUM

AIR LOAD DISTRIBUTIONS ON A FLAPPED WING RESULTING FROM

LEADING-EDGE AND TRAILING-EDGE BLOWING

By H. ^{Neil} Clyde McLemore ✓

Langley Aeronautical Laboratory
Langley Field, Va.

LIBRARY COPY

JUN 10 1957

LANGLEY AERONAUTICAL LABORATORY
LIBRARY, NACA
LANGLEY FIELD, VIRGINIA

CLASSIFIED DOCUMENT

This material contains information affecting the National Defense of the United States within the meaning of the espionage laws, Title 18, U.S.C., Secs. 793 and 794, the transmission or revelation of which in any manner to an unauthorized person is prohibited by law.

NATIONAL ADVISORY COMMITTEE FOR AERONAUTICS

WASHINGTON

June 5, 1957

CLASSIFICATION CHANGED

UNCLASSIFIED

To: *Mr. Pa-1*
By authority of: *Spencer*
Date: *9/17/58*
456

~~CONFIDENTIAL~~

UNCLASSIFIED



NATIONAL ADVISORY COMMITTEE FOR AERONAUTICS

RESEARCH MEMORANDUM

AIR LOAD DISTRIBUTIONS ON A FLAPPED WING RESULTING FROM
LEADING-EDGE AND TRAILING-EDGE BLOWING

By H. Clyde McLemore

SUMMARY

Results of recent wind-tunnel pressure-distribution tests on a large-scale boundary-layer-control model with a 49° sweptback wing have indicated that blowing air at low blowing rates over highly deflected trailing-edge flaps does not produce any unusual flap-load or wing-load problems at low speed. Blowing at very high momentum rates, however, produces large increases in flap loads and extremely high local negative pressures over the flap leading edge.

INTRODUCTION

The current and proposed fighter airplanes having thin highly loaded wings of low aspect ratio place imposing demands on suitable high-lift devices for acceptable low-speed performance. Conventional leading-edge and trailing-edge-flap combinations have proved in wind-tunnel and flight tests (refs. 1 to 3) to be inadequate in this respect in many cases. Serious consideration has been given to methods for achieving additional lift augmentation by boundary-layer control or even to concepts of utilizing a large portion of the powerplant thrust for developing additional lift at low flight speeds.

The boundary-layer-control method, which utilizes only sufficient blowing energy to prevent flow separation, can be expected to achieve, as a maximum, the ideal fluid loading of a given wing configuration with flaps. The concept of utilizing a large amount of engine thrust for lift augmentation, however, introduces the design concepts for short take-off and landing and vertical take-off and landing.

This paper presents an initial wind-tunnel pressure-distribution exploration of lift augmentation by blowing and primarily covers a boundary-layer-control system for a fighter-type airplane. Some of the problems associated with heavily loaded flaps, however, are discussed with a view toward determining the effects of very high momentum blowing rates on the flap loads.

~~CONFIDENTIAL~~

The model used in this investigation was a large-scale wing-body-tail configuration. The wing was swept back 49° at the leading edge and had an aspect ratio of 3.5, a taper ratio of 0.3, and NACA 65A006 airfoil sections streamwise.

Chordwise pressure distributions were obtained at spanwise stations of $0.31b/2$, $0.56b/2$, $0.76b/2$, and $0.90b/2$; however, only the data obtained at the $0.56b/2$ station are presented herein. Tests of this investigation were conducted at a Reynolds number of 5.2×10^6 which corresponds to a Mach number of 0.08.

SYMBOLS

C_L	lift coefficient
c	wing chord
c_f	flap chord
$c_{n,f}$	flap section normal-force coefficient
$C_{\mu,f}$	flap blowing momentum coefficient, $wV_j/gq_\infty S$
$x_{cp,f}$	flap chordwise center of pressure, percent flap chord
c_p	section pressure coefficient
x	distance along wing chord, measured from leading edge
w	weight flow of slot ejected air, lb/sec
V_j	velocity of slot ejected air
g	acceleration due to gravity
q_∞	free-stream dynamic pressure
A	aspect ratio
b	wing span
λ	taper ratio
S	wing area
B.L.C.	boundary-layer control

Subscript:

MAX maximum

DISCUSSION

The geometric characteristics of the large-scale pressure-distribution model and a general description of the wing configurations to be discussed are presented in figure 1. The 24-percent-chord flap extends over 50 percent of the semispan. The leading-edge flow-control devices were a 15-percent-chord slat and a 17-percent-chord droop. The drooped-nose configuration incorporated a blowing slot at the "knee" of the droop, formed by the transition curvature between the drooped nose and the wing upper surface.

The three wing configurations of figure 1 were selected because they represent three relatively good landing configurations from the viewpoint of having the largest possible values of lift coefficient commensurate with acceptable longitudinal stability characteristics up to the stall. For configuration I, a 60-percent-span slat was the largest spanwise extent that would produce longitudinal stability at maximum lift. With flap blowing applied, a full-span leading-edge device is required to maintain the lift effectiveness to high angles of attack; therefore, configuration II incorporated a full-span slat. Configuration III is an alternate method of maintaining the lift effectiveness to high angles of attack.

For the nonblowing configuration (configuration I) the trailing-edge flap was deflected 40° . With flap blowing applied, however, the flap was deflected 60° . The leading-edge slat and the leading-edge droop were deflected 33° and 45° , respectively, measured normal to the wing leading edge.

The chordwise pressure distributions at station 2 ($0.56b/2$) for configurations I and II at a constant value of lift coefficient of 1.27 are shown in figure 2. The flap blowing rate used for configuration II was only sufficient to prevent flow separation over the flap through the lift range. The blowing flap of configuration II experienced a significant increase in load as compared with the nonblowing case, and the blowing also induced some additional load over the rear portion of the wing chord. It should be noted that the most significant loading phenomenon is the large local surface load over the flap, especially in the region of the flap leading edge.

The load on configuration I is concentrated near the wing leading edge in a normal manner. With flap blowing applied, however, the center of load is seen to be concentrated more toward the rear portion of the wing chord.

The chordwise pressure distribution of configuration II of figure 2 is compared in figure 3 with the chordwise pressure distribution of configuration III at the same lift coefficient of 1.27. Configuration III has drooped-nose-knee and trailing-edge-flap blowing in an amount only sufficient to control flow separation through the lift range. Mainly because of the absence of a flow-control device located ahead of the wing leading edge, configuration III has the center of load concentrated still farther rearward.

Although one effect of flap blowing is to move the wing chordwise center of pressure rearward, which would require somewhat larger tail balancing loads, experiments have shown that a tail of normal tail-volume coefficient suitably located with respect to the wing downwash field and operating within its low-speed lift capabilities could supply these additional balancing loads.

The spanwise center-of-pressure characteristics of configurations I, II, and III are not presented in this paper. It has been determined, however, that the maximum spanwise center-of-pressure movement caused by flap blowing was a maximum outboard movement at $C_L = 1.27$ of about 3 percent of the semispan. This outboard movement was no greater than that experienced by the nonblowing configuration at lift coefficients of the order of 0.8. Flap blowing, therefore, should not introduce additional low-speed wing-root bending moments.

Probably the most significant information is presented in figures 4 to 6. The chordwise pressure distribution (station 2) of configuration III at an angle of attack of 12.5° for a wide range of flap blowing rates is shown in figure 4. The blowing momentum coefficient $C_{\mu,f}$ of 0.031 is representative of the boundary-layer-control case; whereas, the value of $C_{\mu,f}$ of 0.187 represents weight-flow rates of the order of 40 to 50 pounds of air per second. If the loading over the flap is observed, it is noted that the flap loads and their contribution to the moment on the rear spar are a function of the blowing momentum. For the boundary-layer-control case ($C_{\mu,f} = 0.031$) the conventional methods of potential-flow calculations are applicable for calculating the section loading characteristics (ref. 4). The other cases shown in figure 4 (the higher blowing rates) have not been examined extensively from the viewpoint of calculating the section loads. The form of these pressure distributions (their smoothness and uniform buildup with increasing blowing rate) suggests, however, that a method can be determined to calculate the section loadings at these high blowing rates.

It should be noted that not only does the load build up over the rear portion of the flap and over the main wing but also an appreciable load buildup occurs over the flap leading edge. The maximum negative pressure

coefficients over the flap leading edge were too large for the higher blowing rates to plot in figure 4; however, the maximum values are listed. For the curve of $C_{\mu,f} = 0.187$, the peak negative pressure coefficient over the flap leading edge was -26.48 .

In order to show the overall perspective of the wing and flap loads for a high flap blowing rate, the curve for $C_{\mu,f} = 0.187$ of figure 4 is shown plotted to a greatly compressed scale in figure 5. The load over the flap is seen to be a large portion of the total load, and the peak negative pressures existing over the flap leading edge are extremely high as compared with the peak pressures existing at the wing leading edge.

In order to obtain a more general, and perhaps more informative, outlook on the significance of these large indicated flap loads with increasing blowing rate, the flap section normal-force coefficients together with the flap centers of pressure for configuration III for a wide range of flap blowing rates are shown as functions of lift coefficient in figure 6.

The flap section normal-force coefficients are seen to increase greatly with increased blowing rate but, as in the case of a normal unseparated flap, increasing lift coefficient has no significant effect on the flap normal-force coefficients. It should be noted here that the large values of $c_{n,f}$ are associated with the large flap blowing rates $C_{\mu,f}$ which are, in turn, inversely proportional to the square of the flight speed, if the momentum of the blowing jet is assumed constant. At relatively high flight speeds the momentum coefficients are small. These high values of $c_{n,f}$ at the high $C_{\mu,f}$ rates are, therefore, necessarily restricted to low to moderate flight speeds in the latter phase of the landing approach and flare.

The flap center of pressure is seen to move toward the flap leading edge with increasing blowing rate because of the high loading over the flap leading edge, and this movement produces some compensating relief of the flap moments. Increasing lift coefficient also has no significant effect on the location of the flap center of pressure.

CONCLUDING REMARKS

The results of wind-tunnel pressure-distribution tests of a large-scale boundary-layer-control model with a 49° sweptback wing indicate that, for the relatively small amount of blowing necessary to prevent flow separation over the flap, no unusual flap-load or wing-load problems are anticipated. When a considerable amount of additional blowing energy

is used, however, large increases in flap loads can be expected; particularly, the loads are extremely high near the flap leading edge and may be the critical design flap load in the landing maneuver.

Langley Aeronautical Laboratory,
National Advisory Committee for Aeronautics,
Langley Field, Va., March 5, 1957.

REFERENCES

1. McLemore, H. Clyde, and Fink, Marvin P.: Blowing Over the Flaps and Wing Leading Edge of a Thin 49° Swept Wing-Body-Tail Configuration in Combination With Leading-Edge Devices. NACA RM L56E16, 1956.
2. Kelly, Mark W., and Tolhurst, William H., Jr.: Full-Scale Wind-Tunnel Tests of a 35° Sweptback Wing Airplane With High-Velocity Blowing Over the Trailing-Edge Flaps. NACA RM A55I09, 1955.
3. Anderson, Seth B., Quigley, Hervey C., and Innis, Robert C.: Flight Measurements of the Low-Speed Characteristics of a 35° Swept-Wing Airplane With Blowing-Type Boundary-Layer Control on the Trailing-Edge Flaps. NACA RM A56G30, 1956.
4. Allen, H. Julian: Calculation of the Chordwise Load Distribution Over Airfoil Sections With Plain, Split, or Serially Hinged Trailing-Edge Flaps. NACA Rep. 634, 1938.

GEOMETRIC CHARACTERISTICS OF LARGE-SCALE
PRESSURE-DISTRIBUTION MODEL

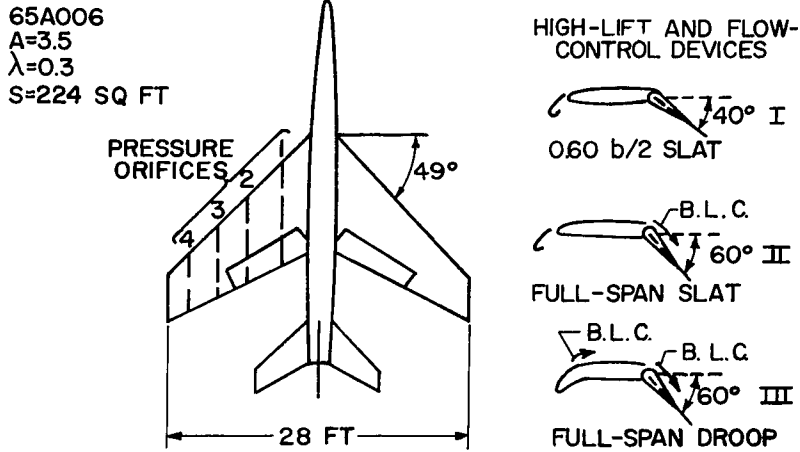


Figure 1

CHORDWISE PRESSURE DISTRIBUTIONS
FOR CONSTANT $C_L=1.27$
EFFECT OF FLAP BLOWING

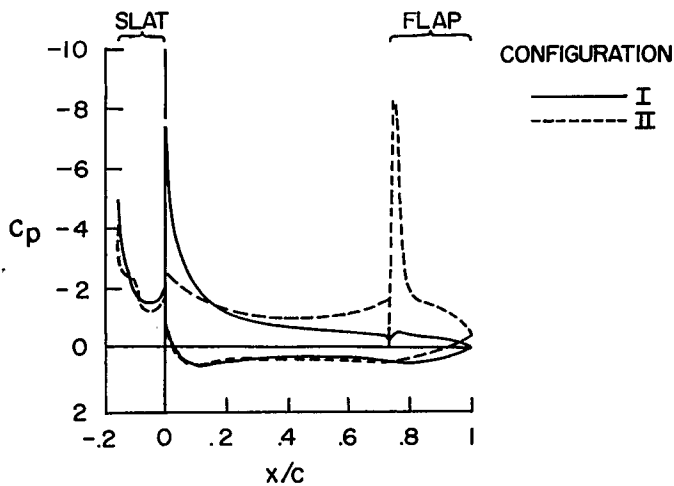


Figure 2

CHORDWISE PRESSURE DISTRIBUTIONS
FOR CONSTANT $C_L=1.27$
EFFECT OF NOSE DROOP

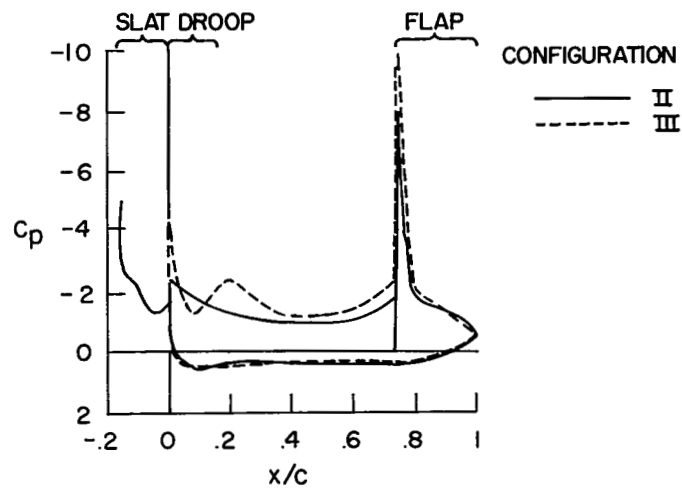


Figure 3

VARIATION OF CHORDWISE PRESSURE DISTRIBUTION WITH
INCREASING FLAP BLOWING
CONFIGURATION III; $\alpha=2.5$

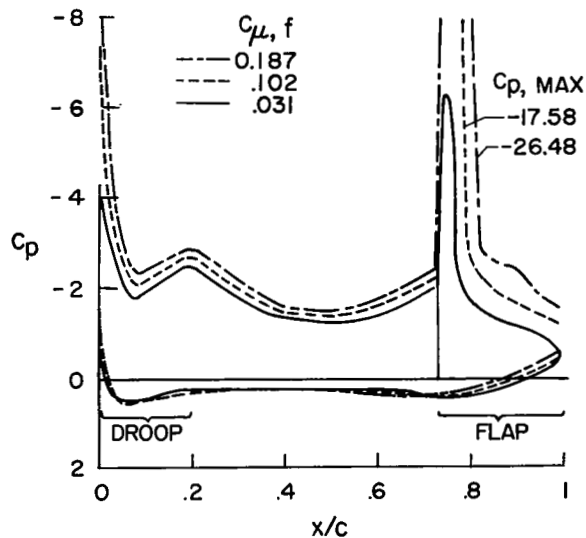


Figure 4

VARIATION OF CHORDWISE PRESSURE DISTRIBUTION
 FOR HIGH MOMENTUM RATE
 CONFIGURATION III; $\alpha = 12.5^\circ$

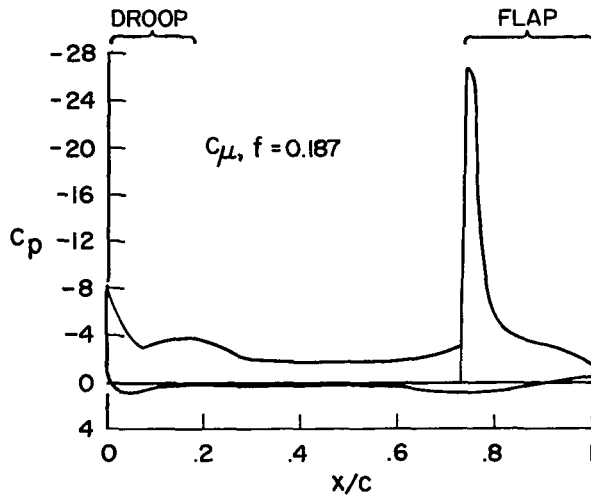


Figure 5

VARIATION OF FLAP NORMAL-FORCE COEFFICIENT AND FLAP
 CENTER OF PRESSURE
 CONFIGURATION III

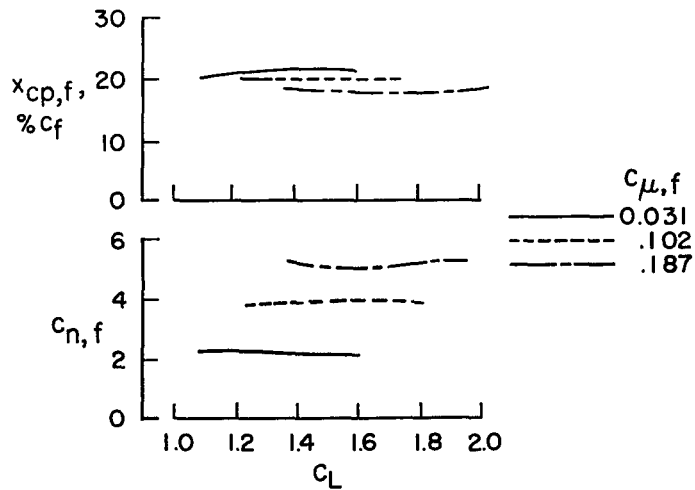


Figure 6

NASA Technical Library



3 1176 01437 9177

